High-Efficiency Joule-Thomson Cryocoolers Incorporating an Ejector

H.S. Cao[1], S. Vanapalli[1], H.J. Holland[1], C.H. Vermeer[2], T. Tirolien[3], H.J.M. ter Brake[1]

[1]University of Twente, 7500 AE, Enschede, The Netherlands
[2]SuperACT, 7559 AJ Hengelo, The Netherlands
[3]European Space Agency, 2200 AG, Noordwijk, The Netherlands

ABSTRACT

Joule-Thomson (JT) cryocoolers have no moving parts and therefore are vibration-free. These are attractive for cooling small optical detectors in space for earth observation missions. JT cryocoolers produce cooling by expanding high-pressure gas through a JT restriction. This, however, is a highly irreversible entropy-generating process. If work could be extracted during the expansion process, the efficiency of the cooling cycle would be significantly improved. In this paper, a JT cooling cycle with an additional ejector is proposed. The high-pressure gas, as the primary fluid of the ejector, is used to compress the low-pressure gas leaving the evaporator, thus reducing the cold-end temperature or/and the input power of the compressor. Compared to a basic JT cycle, the improvement in the COP of the cycle with an ideal ejector is analyzed. The effects of frictional and mixing losses on the real performance of an ejector are estimated through numerical simulations, which aids the understanding of ejector theory and provides information for optimizing the ejector under certain operating conditions.

INTRODUCTION

Joule-Thomson cryocoolers have been used in many applications including cooling of infrared detectors and high-electron-mobility transistor-based devices in space [1], low-noise amplifiers for radio telescopes [2], and cryosurgery [3], among others due to their special features such as compact geometry and absence of moving parts. In a normal JT expansion process, the energy of the high-pressure gas is converted into directed kinetic energy, which is not utilized as work or discharged, but instead is dissipated as heat. This cancels out a large amount of the expansion cooling potential in the gas. Only the Joule-Thomson cooling effect below the inversion temperature remains. Ejectors can use the directed kinetic energy, which is completely wasted in the normal JT expansion, to entrain and compress the low-pressure gas to an intermediate pressure.

Ejectors can be used to reduce the pressure of the evaporator and thereby lower the temperature of the evaporator. Alternatively, ejectors can be used to lift the pressure of the evaporator to a medium pressure and thus reduce the required pressure ratio of the compressor, resulting in less required work of compression. Therefore, an ejector can be used either to lower the pressure (temperature) of the evaporator of a JT cooler, or boost the outlet pressure of a JT cooler. The use of an ejector in a JT cryocooler was first proposed by Rietdijk [4] to create subatmospheric pressure in a

Cryocoolers 19, edited by S.D. Miller and R.G. Ross, Jr.

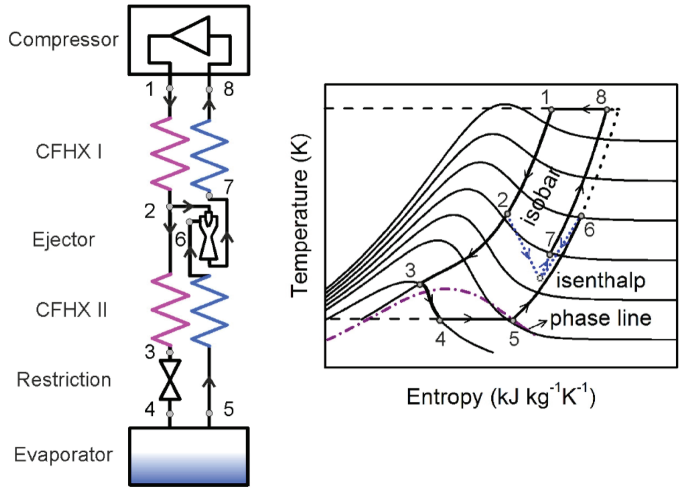

Figure 1. Schematic of Linde-Hampson cycle with an ejector (left) and corresponding temperature versus entropy diagram (right).

liquid helium evaporator. Daney et al. [5] added an ejector to a JT cryocooler with nitrogen gas as the working fluid. An assemble type ejector was used to characterize the performance of an ejector at different dimensions. Both the primary nozzle and the mixing tube-diffuser were exchangeable. There were three primary nozzles with diameters of 0.58, 0.57 and 0.46 mm and three secondary nozzles with diameters of 6.35, 7.54 and 8.73 mm. Several combinations were tested and the best ejector gave a suction pressure of 0.27 bar and an associated saturation temperature of 67.7 K. Most recent studies regarding the use of ejectors in JT cycle systems are on thermodynamic analysis [6, 7]. Very few of these were experimentally verified. It is known that the performance of an ejector not only depends on the system operating conditions (pressure and environment temperature), but also on its geometry and the working fluid. Many researchers have tried to investigate and describe the flow in an ejector in order to develop a high performance ejector [8-10]. However, not all mysteries in the operation of an ejector have been completely cleared. In this paper, the performance improvement of a JT cooler resulting from the addition of an ejector is analyzed. In order to design a JT cooler with an ejector, its performance under certain operating conditions is simulated by means of dynamic modeling. The effects of the operating conditions and the geometry on the ejector performance are discussed.

OPERATING PRINCIPLE

Figure 1 shows the schematic of a Linde-Hampson cycle with an ejector and corresponding temperature versus entropy diagram. In the cycle, the high-pressure gas flows through the counter flow heat exchanger I (CFHX I), then is split into two streams (at point 2). One stream flowing through CFHX II is expanded through the restriction (between points 3,4) and the other stream flows to the ejector as the so-called primary flow. In the ejector, the high-pressure gas (the primary fluid) expands through the nozzle to create low pressure, and then mixes with the secondary fluid from the CFHX II (at point 6) in the mixing section. The mixed gas increases in pressure in the diffuser section and flows to the CFHX I at the medium pressure (at point 7), rather than at the low pressure of the evaporator.

Figure 2a shows a schematic of a typical ejector, which consists of a nozzle, a suction chamber, a mixing section, and a diffuser. A high-pressure primary flow expands in the nozzle where its internal energy and pressure related work convert to kinetic energy. It flows out with supersonic speed to create a very low pressure region at the nozzle exit. Hence, a pressure difference between the streams at the nozzle exit plane and the secondary flow inlet is established and the secondary

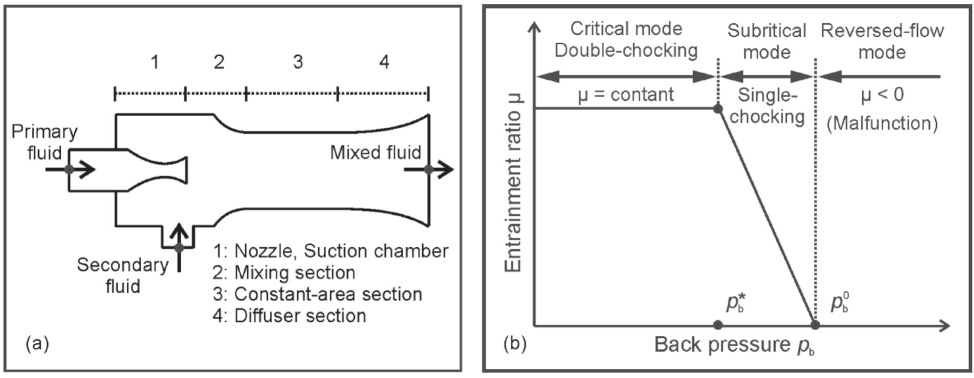

Figure 2. The schematic (a) and operational modes (b) of an ejector [7].

fluid is drawn in by the entrainment effect. In the mixing section, the velocity of the primary flow is slowed down while the secondary flow is accelerated. In the diffuser, the kinetic energy is converted into pressure related flow work.

Figure 1 shows the schematic of a Linde-Hampson cycle with an ejector and corresponding temperature versus entropy diagram. In the cycle, the high-pressure gas flows through the counter flow heat exchanger I (CFHX I), then is split into two streams (at point 2). One stream flowing through CFHX II is expanded through the restriction (between points 3,4) and the other stream flows to the ejector as the so-called primary flow. In the ejector, the high-pressure gas (the primary fluid) expands through the nozzle to create low pressure, and then mixes with the secondary fluid from the CFHX II (at point 6) in the mixing section. The mixed gas increases in pressure in the diffuser section and flows to the CFHX I at the medium pressure (at point 7), rather than at the low pressure of the evaporator.

Figure 2a shows a schematic of a typical ejector, which consists of a nozzle, a suction chamber, a mixing section, and a diffuser. A high-pressure primary flow expands in the nozzle where its internal energy and pressure related work convert to kinetic energy. It flows out with supersonic speed to create a very low pressure region at the nozzle exit. Hence, a pressure difference between the streams at the nozzle exit plane and the secondary flow inlet is established and the secondary fluid is drawn in by the entrainment effect. In the mixing section, the velocity of the primary flow is slowed down while the secondary flow is accelerated. In the diffuser, the kinetic energy is converted into pressure related flow work.

The performance of an ejector is characterized by the entrainment ratio (μ), defined as the ratio of secondary mass flow rate to primary mass flow rate ($\dot{m}_s/\dot{m}_p$), and by the pressure lift ratio (τ), defined as the ratio of the back pressure (p_b, at the exit of the ejector) to the secondary flow pressure (p_s, at the secondary-fluid inlet). Neglecting pressure drops in the CFHXs, this ratio of the inlet pressure of the compressor to the pressure of the evaporator (p_8/p_5) as shown in Figure 1. For a fixed-geometry ejector, the effect of the back pressure on the entrainment ratio is illustrated in Figure 2, in which three regions can be identified: double-choking flow, single-choking flow and reversed flow regions. If the back pressure is below the critical value (p_b^*), the primary flow and the secondary flow are both choked, causing constant entrainment ratio. However, if the back pressure is above the critical value, the entrainment ratio μ will drop sharply with increasing back pressure due to the absence of secondary flow choking. Further increase in back pressure higher than p_b^0 will lead to reversed flow.

The cold-end temperature of a JT cryocooler with an ejector is determined by the boiling temperature of the working fluid at the evaporator pressure. The cooling power $\dot{Q}$ of the cryocooler (shown in Figure 1) is defined by:

$$\dot{Q} = \dot{m}_s \cdot (h\langle T_5, p_5, x_5\rangle - h\langle T_4, p_4, x_4\rangle) \tag{1}$$

where h and x are the specific enthalpy and gas mass fraction, respectively.

Neglecting the heat losses in CFHX I, CFHX II and the ejector, the cooling power $\dot{Q}$ of the cryocooler can also be determined by the change in enthalpy of the working fluid at the warm end of the crycooler:

$$\dot{Q} = \left(\dot{m}_s + \dot{m}_p\right) \cdot \left(h\langle T_8, p_8\rangle - h\langle T_1, p_1\rangle\right) \tag{2}$$

The minimum required power ($\dot{W}$) for a reversible and isothermal compression can be calculated as the change in Gibbs free energy of the fluid during compression:

$$\dot{W} = \left(\dot{m}_s + \dot{m}_p\right) \cdot \left[T_1\left(s\langle T_1, p_1\rangle - s\langle T_8, p_8\rangle\right) - \left(h\langle T_1, p_1\rangle - h\langle T_8, p_8\rangle\right)\right] \tag{3}$$

where s is the specific entropy.

The COP of a cooler is defined as the ratio of the cooling power and the required compressor input power:

$$COP = \dot{Q}/\dot{W} \tag{4}$$

Substituting equations 2 and 3 into equation 4, and equation 4 becomes:

$$COP = \left(h\langle T_8, p_8\rangle - h\langle T_1, p_1\rangle\right)/\left[T_1\left(s\langle T_1, p_1\rangle - s\langle T_8, p_8\rangle\right) - \left(h\langle T_1, p_1\rangle - h\langle T_8, p_8\rangle\right)\right] \tag{5}$$

The cold-end temperature of a JT cryocooler depends on the evaporator pressure (p_5), and the inlet pressure of the compressor equals the product of the evaporator pressure and the pressure lift ratio: $p_5\tau$. The secondary mass-flow rate equals the product of the primary mass-flow rate and the entrainment ratio: $\dot{m}_p\mu$. The outlet pressure of the compressor and the ambient temperature are assumed to be p_h and T_h. CFHX I and CFHX II are assumed to be ideal heat exchangers, which implies that $T_8 = T_1$, and $T_6 = T_2$. Replacing p_1, T_1, p_8 *and* $\dot{m}_s$ by p_h, $T_h, p_5\tau$ *and* $\dot{m}_p\mu$, equations 2 and 5 become:

$$\dot{Q} = \left(\dot{m}_p\mu + \dot{m}_p\right) \cdot \left(h\langle T_h, p_5\tau\rangle - h\langle T_h, p_h\rangle\right) \tag{6}$$

$$COP = \left(h\langle T_h, p_5\tau\rangle - h\langle T_h, p_h\rangle\right)/\left[T_1\left(s\langle T_h, p_h\rangle - s\langle T_h, p_5\tau\rangle\right) - \left(h\langle T_h, p_h\rangle - h\langle T_h, p_5\tau\rangle\right)\right] \tag{7}$$

Equation 6 shows that the cooling power is determined by the change in enthalpy of the working fluid due to isothermal compression at ambient temperature, as is the case in a basic JT cooler without an ejector. The COP of a basic JT cooler operating under the same conditions (compressor outlet pressure p_h, compressor temperature T_h and evaporator pressure p_5) would be:

$$COP_0 = \left(h\langle T_h, p_5\rangle - h\langle T_h, p_h\rangle\right)/\left[T_1\left(s\langle T_h, p_h\rangle - s\langle T_h, p_5\rangle\right) - \left(h\langle T_h, p_h\rangle - h\langle T_h, p_5\rangle\right)\right] \tag{8}$$

Figure 3 shows the effect of the pressure lift ratio on the COP of the JT cryocooler when it is equipped with an ejector. The cryocooler is operated with nitrogen and methane at different cold-end temperatures. The outlet pressure of the compressor and the ambient temperature are assumed to be 8.0 MPa and 295 K, respectively. The COP at the pressure lift ratio of 1 is that of a basic JT cryocooler operating under the same conditions. Compared to a basic JT cryocooler, the COP of a JT cryocooler with an ejector is higher because the pressure of the evaporator (p_5) is compressed to a higher pressure ($p_5\tau$) by the ejector. Thus less input power is required to compress the working fluid to a pressure p_h.

Figure 4 shows the entrainment ratio as a function of the temperature in point 7 shown in Figure 1 at a fixed pressure lift ratio. In this analysis, nitrogen gas is considered as the working fluid and the evaporator pressure is 0.050 MPa in order to achieve a cold-end temperature of 71.8 K. The outlet and inlet pressures of the compressor are selected as 8.0 and 0.1 MPa with a fixed pressure lift ratio of 2.0. Based on energy conservation, the entrainment ratio increases as the temperature of point 7 increases from 100 to 295 K. Since a relatively low entrainment ratio is easier to realize, Figure 4 suggests that it is attractive to place the ejector at a relatively low temperature. However, at low temperature the working fluid may condense and the resulting two-phase flow may disturb the performance of the ejector. This topic is currently under investigation.

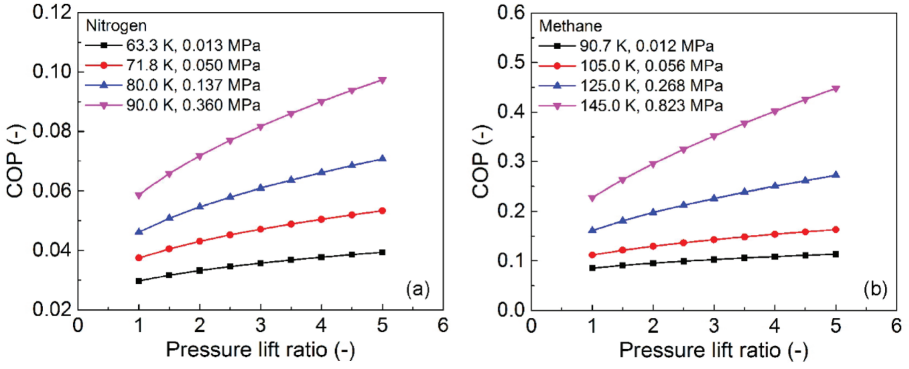

Figure 3. COP of a JT cryocooler with an ejector operating with nitrogen (a) and methane (b) at different cold-end temperatures as a function of the pressure lift ratio (p_1 = 8.0 MPa and T_h = 295 K). The evaporator pressures are the saturation pressures at corresponding cold-end temperatures.

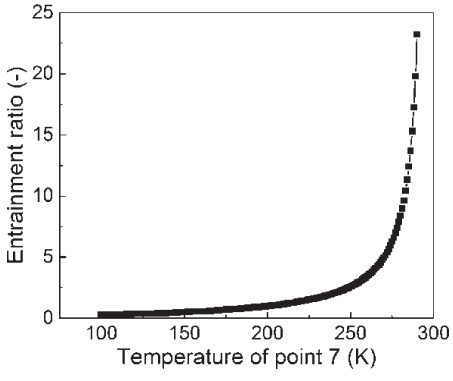

Figure 4. Entrainment ratio as a function of temperature of point 7 shown in Figure 1 (p_1 = 8.0 MPa; p_5 = 0.05 MPa, p_8 = 0.1 MPa and T_h = 295 K).

MODELLING OF AN EJECTOR

In order to design a JT cooler with an ejector, the ejector performance at different conditions needs to be investigated. There are typically two ways for simulating the flow process in an ejector: thermodynamic modeling and dynamic modeling [11]. Thermodynamic modeling uses a one-dimensional model, in which the state and operating parameters of a few sections along the ejector are obtained through steady-state governing equations. Detailed velocity, pressure, and temperature distributions along the ejector are not considered. The effects of frictional and mixing losses are taken into account by using corresponding coefficients introduced in the governing equations. However, these coefficients need to be determined experimentally or by using a dynamic model. The dynamic model is a three-dimensional model, by which detailed information such as velocity, pressure, and temperature distributions along the ejector can be obtained. Besides, the position of the shock waves can also be tracked.

In this study, dynamic models are adopted to simulate the flow process in ejectors with nitrogen gas in order to investigate the performance of ejectors at different operating conditions. Dynamic models are expressed in differential equations (continuity, momentum and total energy), which are solved by using numerical methods, such as finite difference method, finite element method, and finite volume method. In this work, the software ANSYS Fluent based on a finite volume approach is used. The flow in the ejector is assumed to be governed by the ideal gas compressible steady-state axisymmetric form. The turbulent behavior was treated using the Reynolds averaging principle (RANS). The standard version of the k-ε turbulence model was chosen in this work [12] [13] [14].

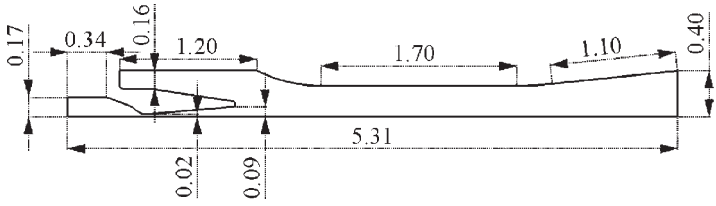

Figure 5. Geometry of the baseline ejector design used in the CFD simulations (mm).

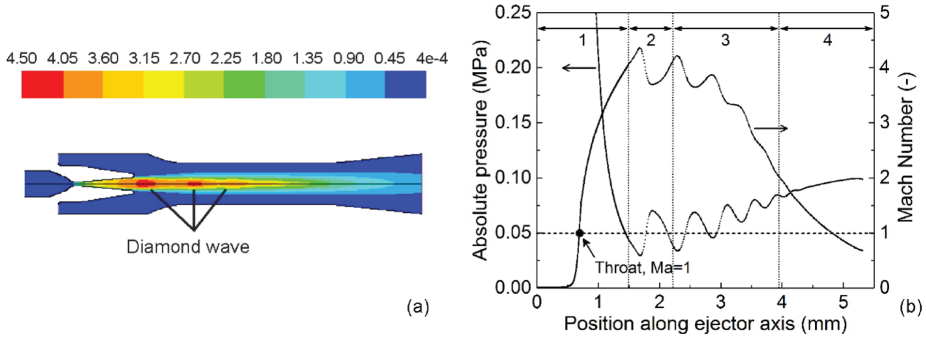

Figure 6. Mach number and absolute static pressure distributions inside the ejector under $p_p = 8.0$ MPa, $T_p = 295$ K, $p_s = 0.05$ MPa, $T_s = 295$ K and $p_b = 0.1$ MPa. (a) Mach number contour; (b) Pressure and Mach number along ejector axis. The four sections are the nozzle, the mixing section, the constant area section and diffuser section as shown in Figure 2a.

The transport equations for the turbulent kinetic energy (k) and the turbulent kinetic energy dissipation rate (ε) can be found in the ANSYS Fluent theory guide [15]. Pressure inlet boundary conditions are used to define the primary and secondary flow inlet pressure, and the outlet of the ejector is assigned to be a pressure outlet boundary condition. Temperature is applied for the inlet and outlet thermal condition, and the ejector wall is set to be adiabatic. Figure 5 shows the geometry of the baseline ejector design used in the CFD simulations. As depicted, the overall size is slightly more than 5 mm, obviously aiming at incorporation in a microcooler.

Figure 6 shows the Mach number and absolute static pressure distributions inside the ejector when the pressures and temperatures of the primary and secondary flows are set at 8.0 MPa, 0.05 MPa and 295 K, and the exit pressure is set at 0.1 MPa. The Mach number reaches 1 at the throat of the nozzle. The Mach number increases to supersonic values with the primary flow expanding to a lower pressure. The "diamond wave" phenomenon manifested by a series of oscillations of the Mach number and the static pressure along the axis of the ejector, is qualitatively consistent with observed laser tomography of Desevaux [16] and CFD investigation of Ji et al [14]. The phenomenon is caused by the large velocity difference between the supersonic primary flow and the entrained secondary flow. As the diamond wave decays the secondary fluid is accelerated and mixed with the primary flow. In the meantime, the static pressure gradually increases to the discharge value and the Mach number reduces to subsonic value.

Figure 7a shows the effect of the back pressure of the ejector on the entrainment ratio with $\dot{m}_p = 25.5$ mg s^{-1} when the pressures and temperatures of the primary and secondary flows are set at 8.0 MPa, 0.05 MPa and 295 K, respectively. Similar to the general relation between entrainment ratio and the back pressure (see Figure 2b), the entrainment ratio is independent on the back pressure when the back pressure does not exceed the critical value ($p_b^* = 0.06$ MPa). When the back pressure is higher than that critical value, the entrainment ratio decreases with increasing back pressure. At $p_b^0 = 0.108$ MPa, the entrainment ratio is zero. Further increase in back pressure will lead to reverse flow.

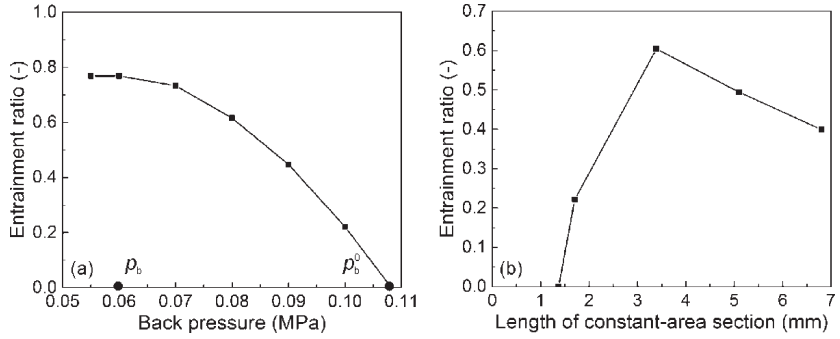

Figure 7. (a): Effect of back pressure and (b): Effect of length of the constant-area section on the entrainment ratio with p_b = 0.1 MPa. (p_p = 8.0 MPa, T_p =295 K, p_s = 0.05 MPa and T_s =295 K).

Figure 7b shows the effect of the length of the constant-area section of the ejector (see Figure 3) on the entrainment ratio with $\dot{m}_p$= 25.5 mg s^{-1} when the pressures of the primary, secondary and discharge flows are set at 8.0 MPa, 0.05 MPa and 0.1 MPa, respectively. The ejector has the dimensions shown in Figure 5 and only the length of the constant-area section is varied. The entrainment ratio increases with increasing length of the section. Figure 6a shows that the primary jet flow core leaves the nozzle exit plane with supersonic speed while the secondary flow outside the jet flow core remains at relatively low speed. The radial non-uniformity in the velocity distribution leads to momentum exchange, which is driven by the combined action of turbulent eddies and interphase drag. To achieve a complete mixing, the length of the momentum exchange (the total length of the mixing section and the constant area section shown in Figure 2) needs to exceed a certain value. However, the losses due to friction effect also increases with increasing total length of mixing section and constant-area section. As shown in Figure 7b, the optimum length under the above-mentioned operating conditions is about 3.4mm.

CONCLUSIONS

The application of an ejector in Joule-Thomson cryocoolers is discussed, and the performance improvement is explained using nitrogen and methane as working fluids. The function of the ejector is to lift the pressure of the evaporator to a medium pressure and thus to reduce the required pressure ratio of the compressor, resulting in less compression work and a higher coefficient of performance. The COP increases with increasing pressure lift ratio. With a given pressure lift ratio, the required entrainment ratio decreases as the ejector shifts from the warm end to the cold end of a cryocooler resulting from energy conservation. The optimum position of the ejector in a JT cycle depends on the ejector performance at certain operating conditions. To investigate that performance, a dynamic model is developed. The effect of the back pressure and the length of the constant area on the ejector performance are investigated at room temperature. The dependence of the entrainment ratio on the back pressure and the length of the constant area is explained. Future work will focus on the simulation of the ejector performance at low temperature with two-phase flow involved, the experimental validation thereof and the actual realization of cryocoolers equipped with ejectors.

ACKNOWLEDGMENT

This work was supported by the European Space Agency (ESA) under Contract No. 4000114493/15/NL/KML/fg.

REFERENCES

1. Collaudin, B. and Rando N., "Cryogenics in space: a review of the missions and of the technologies," *Cryogenics*, vol. 40, no. 468 (2000), pp. 797-819.

2. Cao, H.S., et al., "Cooling a low noise amplifier with a micromachined cryogenic cooler," *Review of Scientific Instruments*, vol. 84, no. 10 (2013), pp. 105102.

3. Fredrickson, K., G. Nellis, and S. Klein, "A design method for mixed gas Joule-Thomson refrigeration cryosurgical probes," *International Journal of Refrigeration*, vol. 29, no. 5 (2006), pp. 700-715.

4. Rietdijk, J.A., "The Expansion-Ejector: A New Device for Liquefaction and Refrigeration at 4 K and lower, " *Liquid Helium Technology, Proceedings of the International Institute of Refrigeration*, Pergamon Press, New York (1966) p. 241.

5. Daney, D.E., McConnell, P.M. and Strobridge. T.R. "Low-Temperature Nitrogen Ejector Performance," *Advances in Cryogenic Engineering*, vol. 18 (1973), pp. 476-485.

6. Yu, J., "Improving the performance of small Joule-Thomson cryocooler," *Cryogenics*, vol. 48, no. 9-10 (2008), pp. 426-431.

7. Rashidi, M.M., Bég, O.A. and Habibzadeh, A. "First and second law analysis of an ejector expansion Joule-Thomson cryogenic refrigeration cycle," *International Journal of Energy Research*, vol. 36, no. 2 (2012), pp. 231-240.

8. Huang, B.J., et al., "A 1-D analysis of ejector performance," *International Journal of Refrigeration*, vol. 22, no. 5 (1999), pp. 354-364.

9. Rusly, E., et al., "CFD analysis of ejector in a combined ejector cooling system," *International Journal of Refrigeration*, vol. 28, no. 7 (2005), pp. 1092-1101.

10. Pianthong, K., et al., "Investigation and improvement of ejector refrigeration system using computational fluid dynamics technique," *Energy Conversion and Management*, vol. 48, no. 9 (2007), pp. 2556-2564.

11. He, S., Y. Li, and R.Z. Wang, "Progress of mathematical modeling on ejectors," *Renewable and Sustainable Energy Reviews*, vol. 13, no. 8 (2009), pp. 1760-1780.

12. Scott, D., Z. Aidoun, and M. Ouzzane, "An experimental investigation of an ejector for validating numerical simulations," *International Journal of Refrigeration*, vol. 34, no. 7 (2011), pp. 1717-1723.

13. Hemidi, A., et al., "CFD analysis of a supersonic air ejector. Part I: Experimental validation of single-phase and two-phase operation," *Applied Thermal Engineering*, vol. 29, no. 8-9 (2009), pp. 1523-1531.

14. Ji, M., et al., "CFD investigation on the flow structure inside thermo vapor compressor," *Energy*, vol. 35, no. 6 (2010), pp. 2694-2702.

15. ANSYS Fluent Theory Guide, 2013: FLUENT Inc.

16. Desevaux, P., "A method for visualizing the mixing zone between two co-axial flows in an ejector," *Optics and Lasers in Engineering*, vol. 35, no. 5 (2001), pp. 317-323.